



## ORIGINAL ARTICLE

# *Millettia ferruginea* extract attenuates cisplatin-induced alterations in kidney functioning, DNA damage, oxidative stress, and renal tissue morphology



Mouna Yassir<sup>a</sup>, Meriam Tir<sup>b</sup>, Afoua Mufti<sup>c</sup>, Anouar Feriani<sup>c</sup>, Bilel Faidi<sup>d</sup>, Nizar Tlili<sup>e,f</sup>, Mansour Sobeh<sup>a,\*</sup>

<sup>a</sup> AgroBioSciences, Mohammed VI Polytechnic University, 43150 Ben-Guerir, Morocco

<sup>b</sup> Laboratoire d'Ecologie, de Biologie et de Physiologie des Organismes Aquatiques, LR18ES41, Faculté des Sciences de Tunis, Université Tunis EL Manar, 2092 Tunis, Tunisia

<sup>c</sup> Laboratory of Biotechnology and Biomonitoring of the Environment and Oasis Ecosystems, Faculty of Sciences of Gafsa, 2112 Gafsa, Tunisia

<sup>d</sup> CHU ibn Eljazar, Unités Chirurgicales les Aglabides Kairouan, Service de Chirurgie Générale, Tunisia

<sup>e</sup> Institut Supérieur des Sciences et Technologies de l'Environnement, Université de Carthage, Tunisia

<sup>f</sup> Faculté des Sciences de Tunis (UR13/ES25), Université Tunis El - Manar, 2092, Tunis, Tunisia

Received 23 March 2022; accepted 7 June 2022

Available online 11 June 2022

## KEYWORDS

*Millettia ferruginea*;  
Inflammatory;  
Oxidative stress;  
Nephroprotective;  
Antioxidant

**Abstract** This study aimed to investigate the beneficial role of *Millettia ferruginea* extract (MF) in preventing cisplatin (Cisp) induced nephrotoxicity in rats. A total of 55 metabolites were identified using LC-MS analysis. The *in vivo* results indicated that MF pretreatment for 4 weeks (20 mg/kg b. w.) remarkably attenuated the altered renal biomarkers by decreasing the levels of plasma creatinine, urea, and uric acid when compared to the Cisp-group. The nephroprotective capacity of MF was further strengthened by histopathological observations, where Cisp + MF treated rats showed lower number of inflammatory cells and tubular degenerative changes than the Cisp-group. The harmful effects of cisplatin on renal oxidative stress indicators (MDA, SOD, CAT, and GPx), were restored by the treatment of MF. In addition, the reduction of inflammatory markers (IL-6 and TNF- $\alpha$ ), associated with alleviating DNA fragmentation, highlighted the preventive effect of MF in kidney tissue. Additionally, MF components presented lower binding energies when docked into the active site of TNF- $\alpha$  and IL-6. The present findings concluded that *M. ferruginea*

\* Corresponding author.

E-mail address: mansour.sobeh@um6p.ma (M. Sobeh).

Peer review under responsibility of King Saud University.



Production and hosting by Elsevier

extract exhibited nephroprotective potential, which may be attributed to its antioxidant and anti-inflammatory properties. Further work is recommended to confirm the current results, explore the involved mechanism of action, and determine the therapeutic doses and time.

© 2022 The Author(s). Published by Elsevier B.V. on behalf of King Saud University. This is an open access article under the CC BY-NC-ND license (<http://creativecommons.org/licenses/by-nc-nd/4.0/>).

## 1. Introduction

The powerful antineoplastic drug, Cisplatin (Cisp), is a widely used medicine for the treatment of several types of cancers including lung, cervical, bladder, ovarian, testicular, and head and neck cancer. However, its dosage and clinical use are very narrowed due to its deleterious side effects including hepatotoxicity, gastrointestinal toxicity, and nephrotoxicity. The latter is observed in 25–35% of adults and 70% of pediatric therapeutic courses (Casanova et al., 2021a; Afsar et al. 2021). The pathogenesis of Cisp damage is multivariate. Cisp induces both types of cell death: apoptosis and necrosis. Apoptosis is accompanied by therapeutic doses while necrosis is associated with higher doses (Casanova et al., 2021a; Afsar et al. 2021). Unlike other DNA detrimental drugs, Cisp selectively destroys non-dividing renal proximal tubule cells (Casanova et al., 2021a; Afsar et al. 2021). It also induces oxidative stress through the propagation of reactive oxygen species such as superoxide anion and hydroxyl radicals and thus disrupts the redox balance and impairs macromolecules via numerous mechanisms like inflammation, cytoplasmic organelle dysfunction, DNA damage, protein denaturation, and peroxidation of membrane lipids (Feriani et al., 2017). To date, there are no clinical active therapeutic agents to treat or prevent Cisp-induced nephrotoxicity. Natural secondary metabolites could ameliorate this disorder due to their multi-target mechanisms including antioxidant and anti-inflammatory (Fang et al. 2021; Rehman et al. 2014; Rehman and Rather, 2019; Erdemli et al. 2021).

The genus *Millettia*, a member of the Fabaceae family, contains 260 species, out of which, 139 species are endemic to Africa. The species are cultivated as trees, climbers, or shrubs and distributed over tropical regions of Asia, Australia, America, and Africa (Buyinza et al. 2020). *Millettia ferruginea* (Hochst.) Baker, commonly known as “berbera” or “brebra” in the local Amharic language, is a tree endemic to Ethiopia. The plant is a livestock feed and its traditional use is limited to wound healing (Choudhury et al. 2016). *M. ferruginea* extracts displayed a plethora of biological activities. These contained antibacterial, antifungal, trypanocidal, larvicidal, antitubercular, anti-cancer and anti-leishmanial potential (Buyinza et al. 2020; Nibret and Wink, 2011). A recent study reported pronounced antimicrobial activities from leaves and bark extracts from Ethiopian flora (Bahiru et al. 2020). Another study highlighted the cytotoxic potential of two isoflavones, isolated from the seeds, ferrugone and 6,7-dimethoxy-3',4'-methylenedioxy-8-(3,3-dimethylallyl)isoflavone against two human ovarian cancer cells (Wang et al. 2020). *M. ferruginea* extracts are rich in isoflavones rotenoids. They occur in almost all plant parts flowers, fruits, seeds, seedpods, roots, stem bark, and grains; however, to date, the chemical

composition of the leaves was not explored (Buyinza et al. 2020). For instance, Choudhury et al. (2016) isolated three secondary metabolites from the seeds namely barbigerone, durmillone, and calopogoniumisoflavone A. The latter was safe and did not show any DNA fragmentation at the therapeutic doses in comet assay.

The present study was aimed to identify the chemical composition of the aerial parts of *M. ferruginea* extract via LC-MS and explore its protective effects, for the first, against cisplatin-induced nephrotoxicity via several biochemical parameters. These include enzymatic antioxidant activities in the kidney (SOD, CAT, and GPx), DNA fragmentation along with the histopathological study. Furthermore, we also determined the antioxidant activities of the extract via DPPH and FRAP assays, and quantified their contents by Folin-ciocalteu method, as well as, performed *in silico* docking in two molecular targets involved in kidney injury.

## 2. Material and methods

### 2.1. Plant material, extraction, HPLC-PDA-MS/MS analysis, and *in vitro* assays

*Millettia ferruginea* aerial parts were air-dried, ground, and extracted using ultrasound-assisted extraction (UAE) using water (15 g × 400 mL) for 15 min under the extraction parameters: 20 Hz, 5C, amplification of the sound wave 30%, and a pulse of 10 s. The extract was filtered using Glass-wool, then centrifuged (6000 rpm, 7 min). The combined filtrates were completely evaporated under reduced pressure using Buchi rotavapor® R-300 (Flawil, Switzerland) yielding a fine dried powder (2.5 g). Chemical composition analysis by LC-MS was performed as previously described (El-Hawary et al. 2020). Total phenolic content (TPC), DPPH, and FRAP assays were performed according to Ghareeb et al. (Ghareeb et al. 2018).

### 2.2. *In silico* activities

To get an insight into the mechanism by which the tested extract ameliorates the deleterious effects of Cisp, we docked the most abundant compounds into the active site of TNF- $\alpha$  and IL-6P, two molecular targets involved in nephrotoxicity. The crystal structures of TNF- $\alpha$  (PDB ID: 2AZ5) and IL-6P (PDB ID: 1ALU) were downloaded from the protein data bank (<https://www.pdb.org>). Molecular operating environment (MOE), 2013.08; Chemical Computing Group Inc., Montreal, QC, Canada, H3A 2R7, 2016 was utilized to perform the docking analysis according to the previously described method (El-Hawary et al. 2020).

### 2.3. *In vivo* assays

#### 2.3.1. *Animals*

Male Wistar rats of identical age, initially weighing around 160 g, were provided from the Central Pharmacy, Tunisia. The rats were placed inside the laboratory (Faculty of Sciences, Gafsa, Tunisia) under controlled temperature ( $24 \pm 2^\circ\text{C}$ ),  $55 \pm 5\%$  relative humidity, and a 12 h light/dark cycle. The animals were fed on a standard chow diet and water *ad libitum*. The protocols were approved by the local Institute Ethical Committee Guidelines. The trials fully conformed to the Guide for the Care and Use of Laboratory Animals. The utmost best was done to minimize the number of rats and lessen the animals' pain.

#### 2.3.2. *Rats' groupings and treatments*

The renal toxicity was prompted by intraperitoneal injection (IP) of cisplatin dissolved in corn oil; the dose used was 13 mg/kg body weight (b.w.) as per previous studies (Domitrović et al. 2013). The extract did not show any sign of toxicity when tested at 200 mg/kg b.w.. A 1/10 dose was used in the current work. The thirty-two rats were divided into 4 groups ( $n = 8$ ): (i) Control: oral treatment with vehicle control containing corn oil, (ii) MF: oral treatment with MF extract dissolved in corn oil at 20 mg/kg b.w., for thirty days, (iii) Cisp: administration of cisplatin (13 mg/kg b.w.), dissolved in corn oil, a single dose (IP) on day 30th, (iv) Cisp + MF: oral treatment with MF extract (20 mg/kg b.w.) for thirty days, in addition to a single dose of Cisp (IP) on day 30th, 1 h after MF administration.

#### 2.4. *Evaluation of kidney weight index*

Upon concluding the experiment, the rats were sacrificed, their renal tissues were excised and cleaned with NaCl solution. The kidney weight index (KWI) was calculated as  $\text{KWI} = \text{kidney weight (KW)}/\text{body weight (b.w.)}$ .

#### 2.5. *Biochemical determinations*

Blood was collected after sacrificing the rats of each group, then centrifuged for 15 min at 2000g to isolate the plasma. The latter was kept at  $-20^\circ\text{C}$  to analyze numerous biochemical parameters, which include markers of renal injury (urea, uric acid, and creatinine) using colorimetric kits (Sigma-Aldrich) according to the manufacturer's protocol.

#### 2.6. *Estimation of oxidative stress markers in the kidney tissues*

The rats' kidney tissues were reaped on ice then washed with normal saline, after which it was homogenized in potassium buffer (0.1 M, pH 7.4). The resultant mix was centrifuged at 12,000 rpm ( $4^\circ\text{C}$ ) for 15 min, thereafter the supernatant was recovered. The antioxidant enzymes (SOD, CAT, and GPx) activities were quantified as before (Flohé and Günzler, 1984; Marklund and Marklund, 1974; Aebi 1984). Following the method of Buege and Aust (1978), the quantification of thiobarbituric acid-reactive substances (TBARS) assessed the lipid peroxidation, respectively. The procedure of Bradford

(1976), was employed to quantify the protein contents in the kidney tissue homogenate.

#### 2.7. *DNA fragmentation assay*

DNA fragmentation analysis of kidney tissue from both the control and experimental animals was conducted. The DNA was isolated using the method of Kanno et al. (2004). This assay was executed according to the method of Sellins and Cohen (1995), by performing electrophoresis of genomic DNA samples on agarose/EtBr gel.

#### 2.8. *Histopathological observations*

A 10% buffered formalin phosphate solution was used to immediately fix the obtained kidney. The latter was embedded next in paraffin, then cut into 5  $\mu\text{m}$  sections and stained using Hematoxylin and eosin (H&E) for histopathological examination. Under a light microscope, the samples were analyzed by assessing the morphological changes. The histopathological alterations of kidney were scored by the semi-quantitative percentage of damaged area as follows: 0: none, 0.5:  $<10\%$  1: 10–25%, 2: 25–50%, 3: 50–70%, and 4:  $>75\%$  (Kim et al. 2016).

#### 2.9. *Statistical analysis*

The data were expressed as mean  $\pm$  standard deviation (mean  $\pm$  SD). The statistical difference between treatment effects was determined *via* the One-Way Analysis of Variance (ANOVA), along with Tukey *post hoc* test to correct for multiple comparisons. The variance between the experimental groups was considered significant at  $p < 0.05$ . GraphPad Prism 6 (GraphPad Software, San Diego, CA) was used to carry out all analyses.

## 3. Results

### 3.1. *Chemical composition and in vitro results*

Chemical profiling of MF, *via* LC-MS, revealed 55 compounds belonging to several classes, mainly phenolic acids and flavonoids (Table 1). The main compounds were quinic acid (2), ferulic acid C glucoside (14), sinapic acid glucoside (21), quercetin pentosyl-rutinoside (45), quercetin pentosyl-glucoside (46), and apigenin pentosyl-glucoside (50). The total chromatogram is represented in Fig. 1. MF furnished high total phenolic content (211 mg gallic acid equivalent/ g extract) when quantified using Folin-Ciocalteu assay and revealed substantial antioxidant activities as well in two common assays (DPPH:  $\text{EC}_{50} = 8.56 \mu\text{g/mL}$ , FRAP: 19.23 mM  $\text{FeSO}_4/\text{mg}$  extract).

### 3.2. *In silico results*

Tumor necrosis factor- $\alpha$  (TNF- $\alpha$ ) is a proinflammatory cytokine produced by cells of the immune system, in addition to other cells, i.e., mesangial cells of the kidney. TNF- $\alpha$  starts as a functional transmembrane protein and gets cleaved by TNF- $\alpha$  converting enzyme (TACE). It then releases into the

**Table 1** Chemical composition of the aqueous extract of *M. ferruginea* (MF).

NO.	Rt		[M-H] <sup>-</sup>	MS/MS
			Proposed compound	
1	1.67	133	115	Malic acid
2	1.91	191	111, 173	Quinic acid
3	2.73	329	153, 197	Syringic acid pentoside
4	3.05	325	163	Protocatechuic acid glucoside
5	3.20	161	99, 101, 143	Umbelliferone
6	3.25	295	161, 179	Caffeoylmalic acid
7	3.68	265	125, 143, 163	Hydroxy ethenylbenzene-protocatechuic acid
8	4.23	195	123, 167	Hydroxycaffeic acid
9	5.45	164	147	Phenylalanine
10	6.46	437	179, 341	Caffeic acid pentosyl-glucoside
11	8.28	353	191	Chlorogenic acid
12	8.64	311	135, 149, 179	Caffeic acid glucoside
13	9.52	355	179, 295, 355	Feruloyl caffeic acid
14	12.86	285	109, 153	Protocatechuic acid pentoside
15	13.58	359	179, 197	Rosmarinic acid
16	13.89	451	289, 405, 433	Epicatechin glucoside
17	14.16	253	87, 121	Benzoic acid pentoside
18	14.67	337	173, 191	<i>p</i> -Coumaroylquinic acid
19	14.93	295	149, 163	<i>p</i> -Coumaric acid pentoside
20	15.08	385	179, 223	Sinapic acid glucoside
21	17.30	491	359	Rosmarinic acid related compound*
22	18.56	577	289, 407, 425	Procyanidin dimer
23	19.33	325	149, 193	Ferulic acid pentoside
24	20.21	353	191	Neochlorogenic acid
25	20.36	369	205, 223	Sinapic acid rhamnoside
26	22.21	353	173, 179	Cryptochlorogenic acid
27	22.89	865	289, 577, 695	Procyanidin trimer
28	23.00	228	132	Methylpentenoyl aspartic acid
29	23.31	457	163, 325	Gallocatechin gallate
30	23.72	399	205, 223	Feruloyl sinapic acid
31	23.87	625	301, 463	Quercetin diglucosides
32	24.76	577	289, 407, 425	Procyanidin dimer
33	25.07	305	97, 149, 225	Gallocatechin
34	25.65	337	163, 191	<i>p</i> -Coumaroylquinic acid
35	25.75	385	205, 223	Caffeoyl sinapic acid
36	26.67	295	135, 179	Caffeic acid derivative
37	27.03	581	269, 287, 563	Eriodictyol pentosyl-glucoside
38	27.33	449	179, 269, 287	Eriodictyol glucoside
39	27.79	389	161, 227	Resveratrol glucoside
40	29.13	593	311, 353, 473	Vicenin-2
41	29.67	771	271, 301, 609	Quercetin triglucosides
42	29.98	865	289, 577, 695	Procyanidin trimer
43	31.14	625	301, 463	Quercetin diglucosides
44	32.38	741	271, 301, 609	Quercetin pentosyl-rutinoside
45	33.76	595	271, 301, 463	Quercetin pentosyl-glucoside
46	36.03	725	255, 285, 593	Kaempferol pentosyl-rutinoside
47	37.15	609	255, 271, 301	Rutin
48	37.52	579	175, 285, 447	Kaempferol pentosyl-glucoside
49	38.58	447	285	Kaempferol glucoside
50	42.08	563	269	Apigenin pentosyl-glucoside
51	42.29	187	125, 169	Ethyl gallate
52	43.56	431	269, 311	Apigenin glucoside
53	45.09	243	125, 175, 225	Unknown
54	48.23	343	161, 269	Glyceryl apigenin
55	53.99	285	175, 241, 285	Kaempferol

\*3-(3,4-Dihydroxyphenyl)-2-[2-[2-(3,4-dihydroxyphenyl)-4,5-dihydroxyinden-1-ylidene]acetyl]oxypropanoic acid.

circulation, where it would be either as a functional free soluble form or it will bind to TNF receptors 1 and 2 (TNRF1 & TNRF2), referred to as markers of the TNF pathway (Lim et al. 2021; Speeckaert et al. 2012). Interleukin-6 (IL-6) is an

inflammatory cytokine that plays part in both types of inflammation, acute and chronic. IL-6 synthesis can be induced by other cytokines involved in inflammation, viral infections, and bacterial infection-associated lipopolysaccharides, such

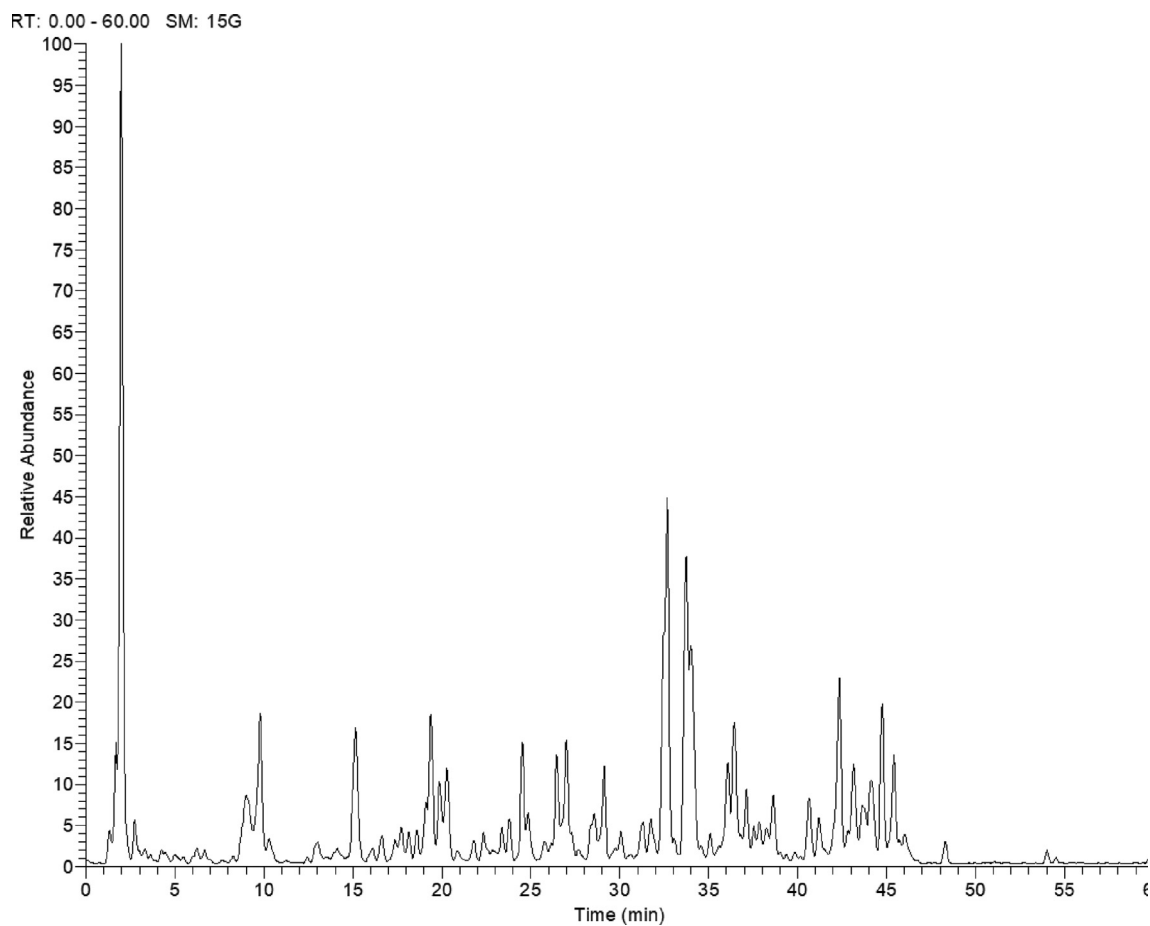


**Fig. 1** *M. ferruginea* (MF) profile using LC-MS.

as TNF- $\alpha$  and IL-1 $\alpha$  (Lim et al. 2021). Chronic kidney disease (CKD) presents a low-grade, persistent, chronic inflammatory state. For instance, it has been verified that Hemodialysis patients' levels of cytokines TNF- $\alpha$  and IL-6 are elevated, due to the size restrictions of traditional dialytic membranes. Thus, the cytokines are not being efficiently cleared. Besides, TNF- $\alpha$  and IL-6 renal and serum levels are reported to be high in experimental kidney disease, viz. cisplatin-induced nephropathy (Lim et al. 2021; Taguchi et al. 2021). Therefore, kidney injuries in which inflammation plays a critical role in the pathogenesis are ameliorated by TNF- $\alpha$  and IL-6 inhibition (Taguchi et al. 2021). *In silico*, MF phytoconstituents provided lower binding energies when docked into the active sites of TNF- $\alpha$ , and IL-6 highlighting their abilities to decrease the production of both markers, Table 2 and Figs. 2 and 3.

### 3.3. In vivo results

#### 3.3.1. MF effects on the body and kidney weights

Fig. 4 illustrates cisplatin and MF effects on the body weight and kidney weights. All the studied groups survived throughout the experimental period. When compared to the control, a significant decline in body weight and a rise in kidney weights were noted in the cisplatin-treated group. Once MF extract

was administered to the treated rats, cisplatin's adverse effects on these parameters were inverted.

#### 3.3.2. MF effect on renal injury markers

The analogy with control rats presented a substantial rise of plasma renal injury markers (creatinine, urea, and uric acid) in Cisp-intoxicated rats, Fig. 5. Pretreatment of MF (20 mg/kg) with Cisp meaningfully reduced the levels of creatinine, urea, and uric acid when compared to the rats to whom Cisp only was administrated. Moreover, the co-treatment of MF, at a dose of 20 mg/kg, without cisplatin resulted in an insignificant difference with the control group.

#### 3.3.3. MF effects on antioxidant biomarkers

The significant increase in MDA levels ( $p < 0.001$ ) indicated oxidative damage in the renal tissue induced upon administration of Cisp (13 mg/kg), Table 3. Treatment with MF (20 mg/kg) caused a significant decline of the elevated MDA levels ( $p < 0.05$ ) compared to the negative control group. However, MF displayed no substantial change in lipid peroxidation compared to the vehicle control group.

Cisp-treated rats exhibited a substantial reduction in the activity levels of CAT, SOD, GPX, and GSH compared with the control group. When comparing the Cisp-treated rats to those who had MF co-administrated with cisplatin, the dam-

**Table 2** Score functions and interactions of MF phytoconstituents in TNF- $\alpha$  and IL-6 active sites using *in silico* modeling.

No.	TNF- $\alpha$		IL-6	
	SF	Interactions	SF	Interactions
51	-6.86	Glu 23 (H bonding)	-13.43	Ser 107 (H bonding)
33	-9.64	Lys 65 (H bonding) Pro 139 (H bonding)	-14.54	Asp 160 (H bonding)
40	-8.65	Lys 65 (H bonding) Glu 23 (H bonding)	-16.40	Arg 104 (H bonding) Glu 106 (H bonding) Asp 160 (H bonding through solvent) Glu 42 (H bonding through solvent) Ser 108 (H bonding through solvent) Gln 159 (H bonding through solvent)
11	-9.47	Lys 65 (H bonding)	-14.36	Arg 104 (Salt bridge) Ser 107 (H bonding)
29	-10.77	Glu 23 (H bonding) Ala 22 (H bonding)	-18.49	Asp 160 (H bonding) Glu 42 (H bonding)
20	-8.69	Glu 23 (H bonding) Lys 65 (H bonding and salt bridge) Asp 140 (Hydrophobic interaction)	-8.56	Glu 42 (H bonding through solvent) Ser 108 (H bonding through solvent) Glu 106 (H bonding)
24	-8.86	Lys 65 (H bonding)	-13.65	Glu 106 (H bonding) Lys 46 (H bonding and salt bridge) Glu 106 (H bonding)
47	-9.55	Ala 22 (H bonding)	-14.33	Asn 103 (H bonding) Glu 42 (H bonding through solvent) Ser 108 (H bonding through solvent) Gln 15 (H bonding through solvent)
55	-7.89	Glu 23 (H bonding) Lys 65 (H bonding)	-9.34	Glu 106 (H bonding) Asp 160 (H bonding)
5	-6.68	Pro 139 (H bonding)	-6.36	Glu 106 (hydrophobic interaction) Ser 107 (H bonding)
12	-7.59	Ala 22 (H bonding) Glu 24 (H bonding)	-11.68	Glu 106 (H bonding) Asp 160 (H bonding)
15	-10.98	Lys 65 (H bonding and salt bridge) Glu 24 (H bonding) Asp 140 (hydrophobic interaction)	-16.17	Glu 106 (H bonding) Arg 104 (Salt bridge) Thr 163 (H bonding through solvent) Asp 160 (H bonding through solvent) Glu 106 (hydrophobic interaction)
31	-10.01	Ala 22 (H bonding) Glu 23 (H bonding) Gln 67 (H bonding) Leu 142 (H bonding) Lys 65 (H bonding)	-14.30	Glu 106 (H bonding) Asp (H bonding) Glu 42 (H bonding through solvent) Ser 108 (H bonding through solvent)
49	-8.42	Pro 139 (H bonding)	-15.06	Arg 104 (H bonding)
8	-9.15	Lys 65 (Salt bridge)	-12.08	Ser 107 (H bonding) Lys 46 (H bonding)
4	-9.59	Pro 139 (H bonding) Lys 65 (H bonding) Gly 24 (H bonding)	-12.55	Ser 107 (H bonding) Lys 46 (H bonding)
38	-8.76	Glu 23 (H bonding) Leu 142 (H bonding) Lys 65 (H bonding)	-14.49	Asp 160 (H bonding) Asn 103 (H bonding)
16	-8.25	Leu 142 (H bonding) Gln 67 (H bonding) Pro 20 (H bonding)	-13.85	Lys 46 (H bonding) Glu 42 (H bonding through solvent) Ser 108 (H bonding through solvent) Gln 159 (H bonding through solvent)
39	-8.47	Leu 142 (H bonding) Ala 22 (H bonding) Gly 24 (H bonding)	-12.80	Asn 103 (H bonding) Gln 159 (H bonding)
22	-10.27	Glu 23 (H bonding) Pro 20 (H bonding) Pro 139 (H bonding) Lys 65 (H bonding and hydrophobic interactions)	-16.90	Glu 42 (H bonding) Arg 104 (H bonding) Thr 163 (H bonding through solvent) Asp 160 (H bonding through solvent) Gln 156 (H bonding through solvent) Ala 153 (H bonding through solvent)

**Table 2** (continued)

No.	TNF- $\alpha$		IL-6	
	SF	Interactions	SF	Interactions
1	-7.63	Lys 65 (H bonding and salt bridge)	-9.32	Glu 106 (H bonding) Arg 104 (Salt bridge)
2	-7.43	Lys 65 (H bonding and salt bridge) Leu 142 (H bonding)	-9.78	Lys 46 (H bonding) Glu 106 (H bonding) Thr 163 (H bonding through solvent) Asp 160 (H bonding through solvent)

Compound numbers are from Table 1. SF: Score function (kcal/mol).

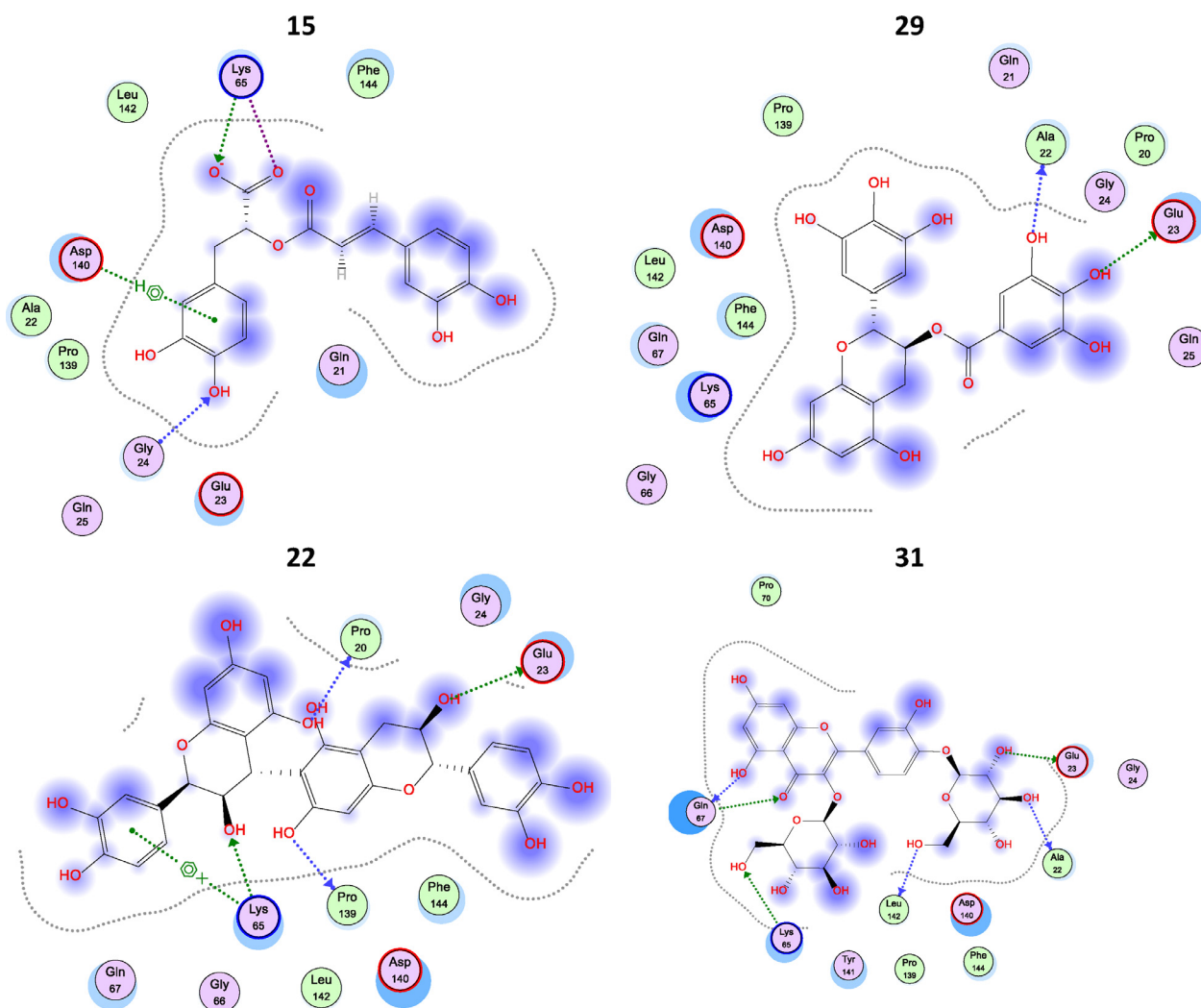


**Fig. 2** 2D representative of selected MF phytoconstituents in TNF- $\alpha$  active site using *in silico* modeling. Compound numbers are from Table 2.

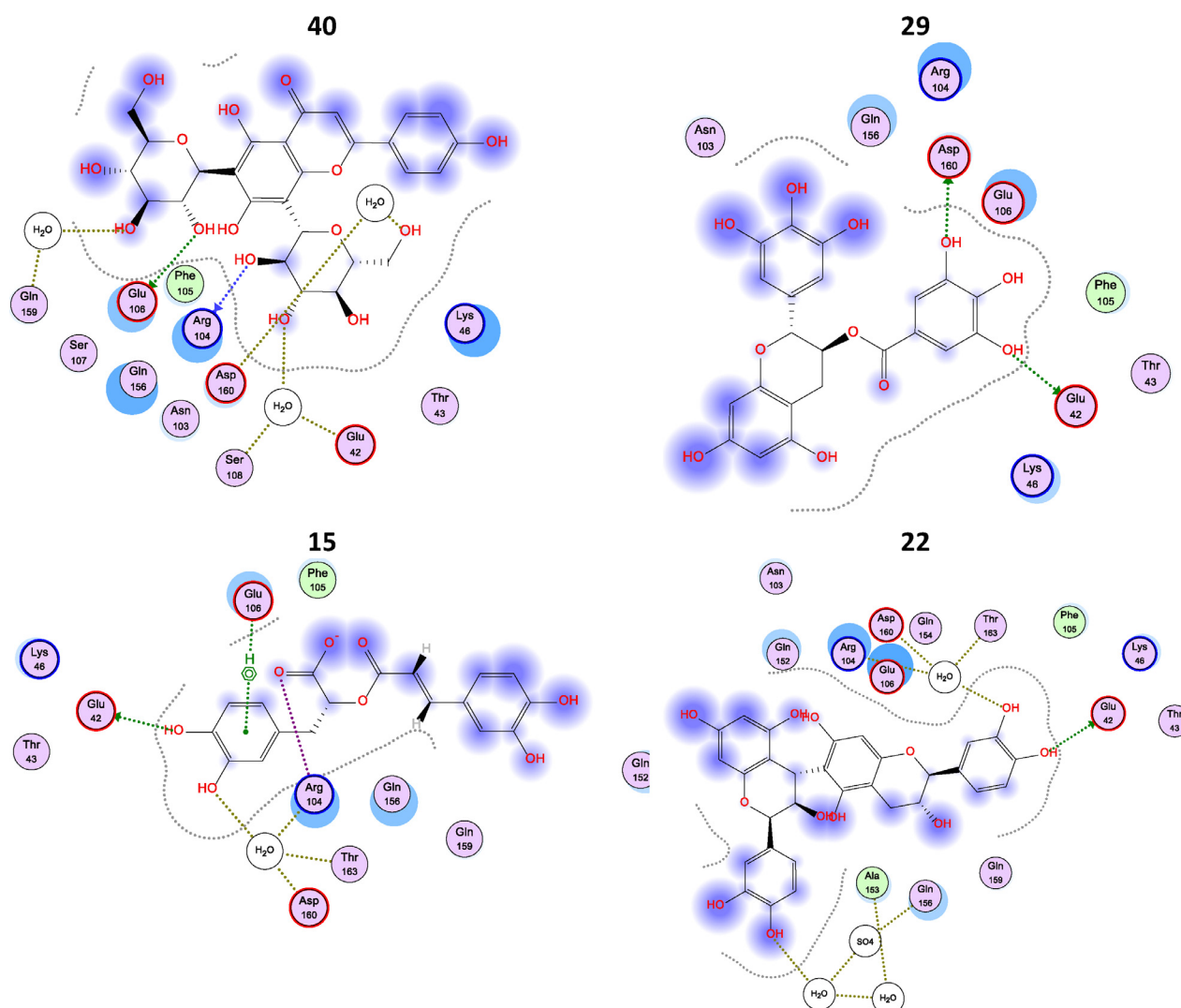


**Fig. 3** 2D representative of selected MF phytoconstituents in IL-6 active site using *in silico* modeling. Compound numbers are from Table 2.

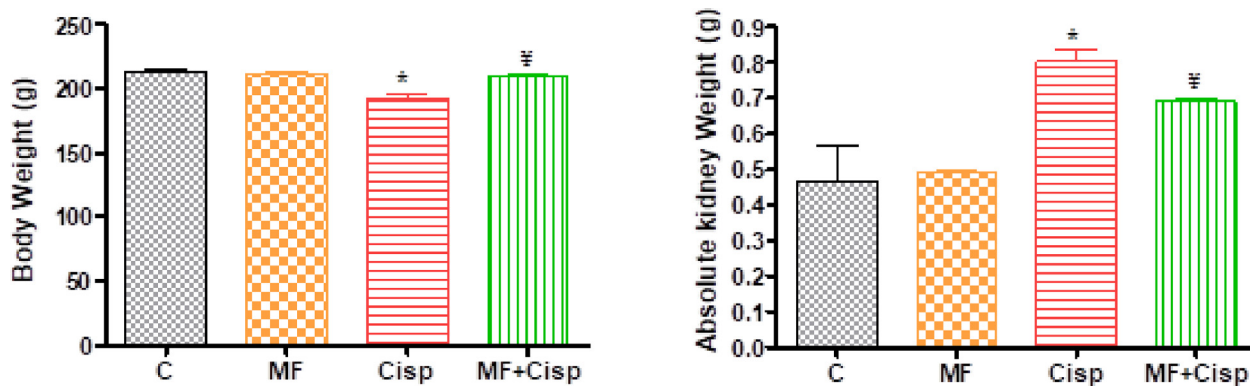


**Fig. 4** Effects of *M. ferruginea* (MF), cisplatin (Cisp), or their combination on body weight and absolute weights of rat kidney in control and experimental groups of rats. Results were expressed as mean  $\pm$  SD of eight rats in each group. \*<sup>Y</sup> $p < 0.05$  significant differences compared to controls and cisplatin group of rats, respectively.

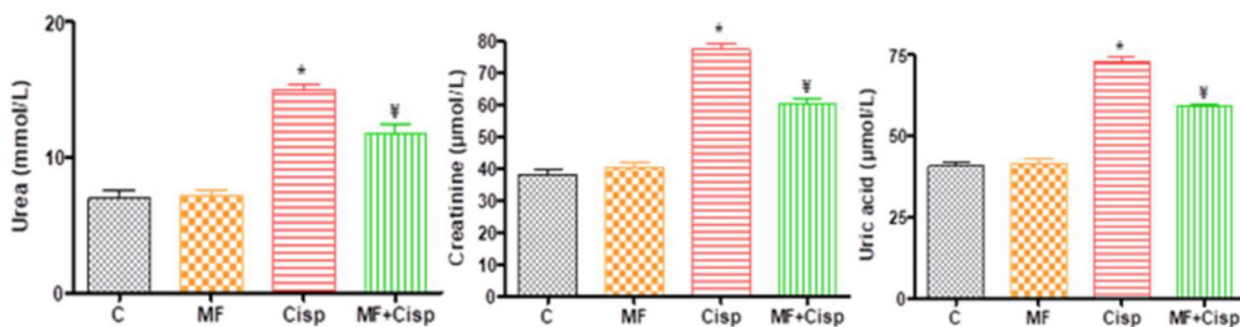


**Fig. 5** Effects of *M. ferruginea* (MF), cisplatin (Cisp), or their combination on plasmatic urea, creatinine, and uric acid in control and experimental groups of rats. Results were expressed as mean ± SD of eight rats in each group. \*, <sup>Y</sup>*p* < 0.05 significant differences compared to controls and cisplatin group of rats, respectively.

**Table 3** The change in TBARS, protein carbonyl (PC), and endogenous antioxidants contents (SOD, CAT, and GPX) in the kidney of different animal groups.

Parameters	Control	MF	Cisp	MF + Cisp
TBARS (nmoles MDA/g tissue)	3.19 ± 0.41	3.87 ± 0.39	10.53 ± 1.13*	7.34 ± 0.89 <sup>Y</sup>
SOD (U/mg protein)	22.65 ± 3.07	23.78 ± 2.84	12.26 ± 2.66*	16.7 ± 2.63 <sup>Y</sup>
CAT (µmol of H <sub>2</sub> O <sub>2</sub> destroyed/min per mg protein)	13.03 ± 1.47	13.42 ± 2.19	6.35 ± 0.81*	9.75 ± 0.81 <sup>Y</sup>
GPx (nmol of NADPH oxidized/min per mg protein)	25.13 ± 3.83	24.72 ± 3.65	14.43 ± 1.28*	19.88 ± 2.09 <sup>Y</sup>

Results were expressed as mean ± SD of eight rats in each group. \*, <sup>Y</sup>*p* < 0.05 significant differences compared to controls and cisplatin group of rats, respectively.

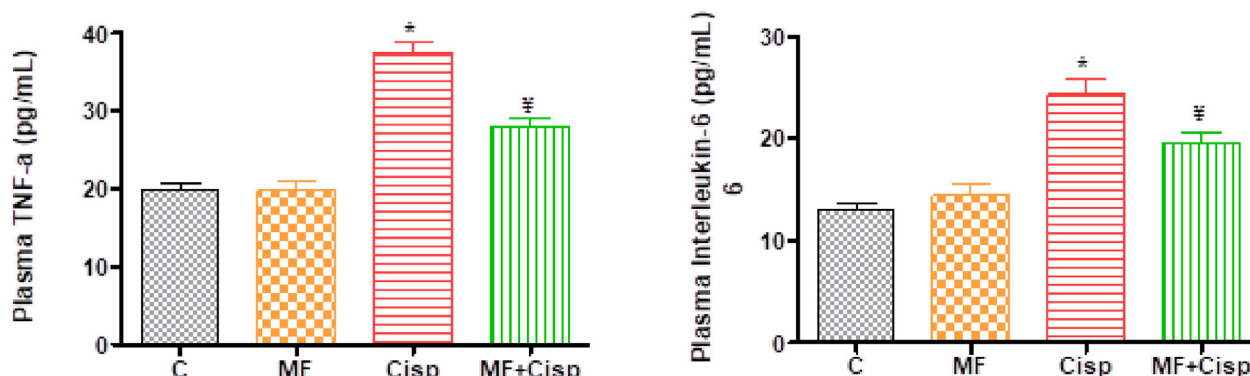


**Fig. 6** Effects of *M. ferruginea* (MF), cisplatin (Cisp), or their combination on Interleukin-6 (IL-6) and TNF-α. Results were expressed as mean ± SD of eight rats in each group. \*, <sup>Y</sup>*p* < 0.05 significant differences compared to controls and cisplatin group of rats, respectively.

aging result on the antioxidant biomarkers was inverted. Prominently, the treatment with MF didn't show a significant difference in the activities of the enzymatic and non-enzymatic antioxidants concerning the control group.

**3.3.4. MF effects on pro-inflammatory cytokines levels**

The treatment with cisplatin (13 mg/kg) induced significantly augmented the inflammatory cytokines (*p* < 0.001), TNF-α, and IL-6 in the plasma, with regard to control rats. As expected, the administration of MF (20 mg/kg) caused a significant reduction of elevated levels of TNF-α and IL-6

(*p* < 0.05) when compared to the control group (Fig. 6 A and B). Nevertheless, when compared to the vehicle control group, MF didn't display any substantial alteration in the levels of inflammatory markers.

**3.3.5. MF effects on the DNA ladder fragmentation in the renal tissue of rats**

The qualitative changes in the integrity of the genomic DNA extracted from the renal tissues are illustrated in Fig. 7. The DNA on the gel electrophoresis demonstrated intact bands for the control samples (lane 1) and the MF-treated ones (lane

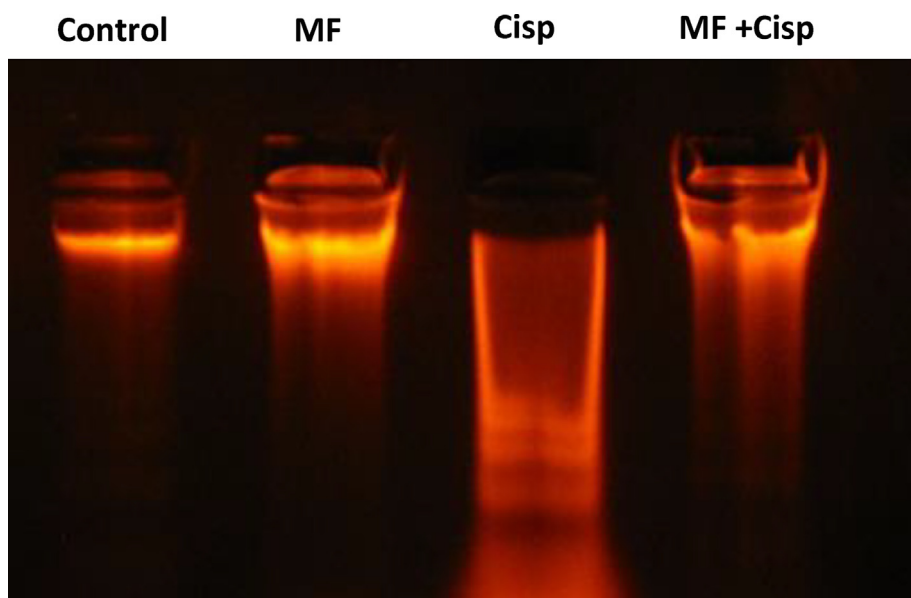


**Fig. 7** Effects of *M. ferruginea* (MF), cisplatin (Cisp), or their combination on agarose gel electrophoresis analysis of cardiac DNA from a different group. Control (Lane 1), MF (Lane 2), Cisp (Lane 3), and MF + Cisp (Lane 4) treated group.

2). On the other hand, an evident degradation, defined by mixed laddering and smearing of the DNA indicating apoptosis was detected in the Cisp-treated samples (lane 3). The Cisp + MF treated samples (lane 4) showed less disintegration and were almost similar to the control samples.

### 3.3.6. Analysis of the renal histology

**Fig. 8(A)** illustrates the H&E staining of renal segments of the entire treated groups. The histologic examination of the renal segments, in both the control and MF group, showed normal architecture of the renal cortex and glomeruli, regular renal tubules, and distinct renal cells. Nonetheless, the analogy between the control and the Cisp group confirms that the latter showed renal tubules atrophy, dilatation of renal tubules, neutrophil infiltration, glomerular atrophy, pyknotic nuclei and multiple foci of hemorrhage indicating renal toxicity. Cisp + MF group demonstrated an auspicious shielding potential of MF against the noxious effect of cisplatin revealed by relatively normal cellular architecture with distinct renal cells. The preventive effect of MF was confirmed by the scoring results as well, **Fig. 8(B)**.

## 4. Discussion

The current study assesses the preventive outcome of *M. ferruginea* (MF) against cisplatin-induced nephrotoxicity in rats and annotated its phytoconstituents. Cisplatin injection significantly increased the kidney weight in rats and pointedly decreased the body weight; this comes in agreement with previous reports ([Sharma et al. 2021](#)); however, MF attenuated this renal hypertrophy. The obtained results also showed elevated amounts of plasma creatinine, urea, and uric acid after cisplatin administration, which corroborates the results stated by [Tir et al. \(Tir et al. 2019\)](#). The significant rise in the plasma

renal failure biomarkers could be linked to the damage of the glomerular function and tubular impairment in the kidneys ([Rjeibi et al. 2018](#)). The optimized H&E staining was used to advocate this proposition. Assuredly, when put through analogy with the control group, the animals intoxicated with cisplatin showed multiple proximal renal tubular damage and cellular necrosis supervened by edema in renal tissue. The pre-coadministration of MF extract restored urea, creatinine, and uric acid levels. The ameliorative role of MF might be related to its bioactive molecules content. In fact, it was previously reported that natural compounds can demonstrate a protective effect upon renal injury ([Dhibi et al. 2016](#); [Konda et al. 2016](#)). Similar research has revealed the possible stabilization of the structural integrity of the kidney cell membrane of bioactive molecules, including quinic acid ([Arya et al. 2014](#)) and syringic acid ([Sancak et al. 2016](#)), which were both identified in MF extract.

Several studies have revealed that cisplatin injection-induced elevated generation of free radicals leads to oxidative stress and changes in the antioxidant defense system of the cells ([Tlili et al. 2017](#)). Lipids, DNA, and proteins can be destroyed by free radical production. Cisplatin intoxication occasioned the reduction of SOD and CAT activities, and GSH content, while it augmented the lipid peroxidation; the aforesaid findings conform to the report of [Hussain et al. \(Hussain et al. 2012\)](#). The abovementioned proves the role of oxidative stress, induced by cisplatin, in inducing nephrotoxic damage. MF administration produced a noteworthy reverse of the oxidative parameters inferring the antioxidant action of MF, in addition to the improvement of nephrotoxicity. MF reduced lipid peroxidation (MDA) with the ensuing enhancement of endogenous antioxidants activities (SOD, CAT, and GPx). The nephroprotection of MF is conferred by its bioactive compounds which can reverse the reactivity of the free radicals into inactive products. Preceding research indicated that lipid peroxidation could be reduced by natural antioxi-

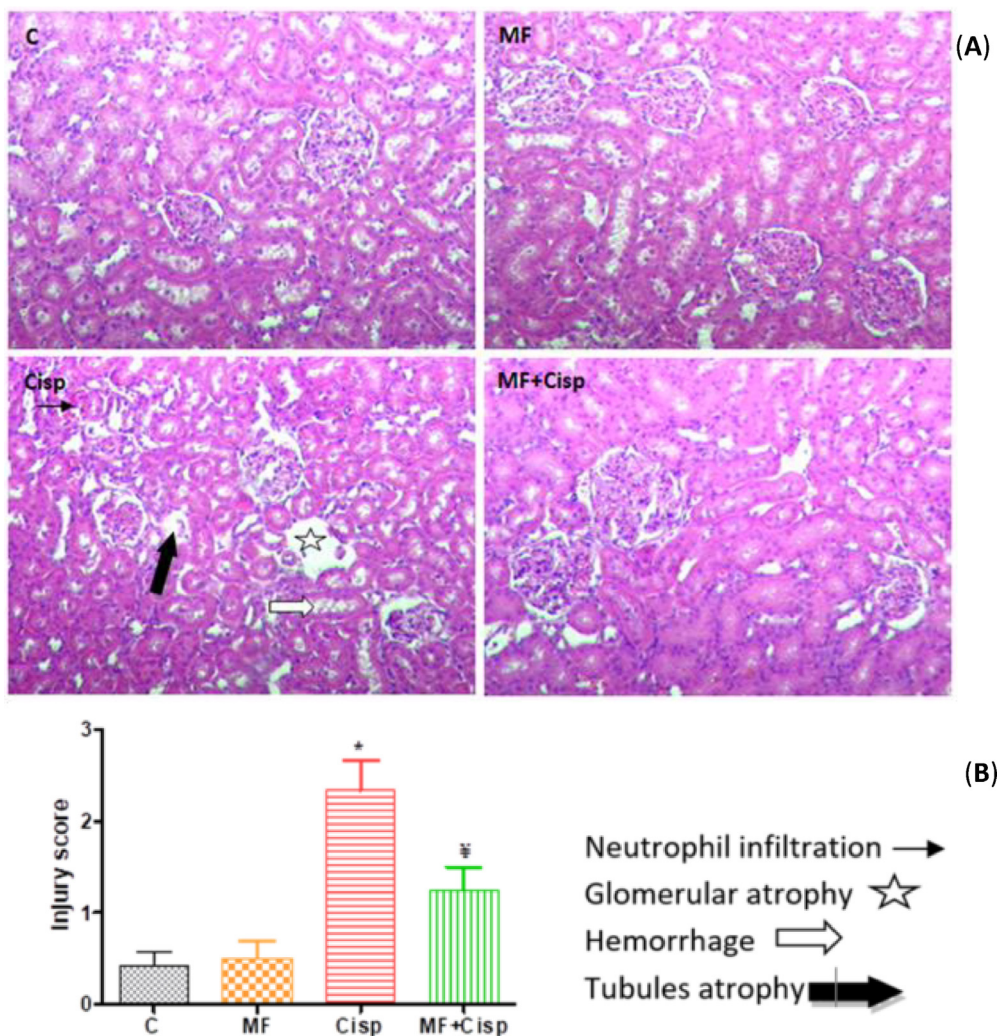


**Fig. 8** Effects of *M. ferruginea* (MF), cisplatin (Cisp), or their combination on histology of kidney sections using hematoxylin and eosin (H and E, 400x) stained rats renal (A) and scored (B) by the semi-quantitative percentage of damaged area. C and MF: Kidney section of a control and MF alone rats showing normal histology of renal parenchyma. Cisp: Kidney section of Cisp treated rats showing the damage induced by Cisplatin. MF + Cisp: Kidney section of MF treated rats showing relatively normal cellular architecture with distinct renal cells.

dants in the kidneys (Sahu et al. 2013). Many reports showed that quinic and syringic acids (identified from the extract) pointedly improved SOD and GSH levels (Arya et al. 2014; Sancak et al. 2016).

Renal cells apoptosis induced by oxidative stress plays a significant role in the progression of renal tissue injury. This hypothesis was strengthened by the present findings revealing that cisplatin injection remarkably induced DNA fragmentation and apoptosis. Interestingly, the pre-cotreatment of MF extract attenuated the DNA damage in kidney tissue, highlighting that MF reduced oxidative stress which resulted in mitigated apoptosis. Several reports highlighted the anti-nephrotoxicity of plant extract in renal tissue (Afsar et al. 2020; Feriani et al., 2017).

Inflammatory cytokines, namely TNF- $\alpha$  and IL-6, are released due to inflammatory cells chemotaxis in acute renal failure. The current study showed high levels of TNF- $\alpha$  and IL-6 implying that the treatment with cisplatin incited the inflammatory pathway, potentially contributing to kidney

damage. The rats treated with Cisp + MF showed lower levels of IL-6 and TNF- $\alpha$  than those supplemented solely with Cisp. These results were also observed *in silico*, several secondary metabolites from the extract bound to the active sites of TNF- $\alpha$  and IL-6 revealed low binding energies. Thus, the tenacity of nephrotoxicity-mediated inflammation decreased. As a matter of fact, the capacity of MF as an antioxidant could be accountable for suppressing the inflammation of the renal cells and reducing the cytokines production and the acute-phase proteins in the blood.

Rosmarinic acid, detected at the extract, prevented the increase of creatinine level, as well as reduced renal and serum MDA levels by 44 and 41%, respectively (El-Desouky et al. 2019). Sinapic acid, annotated at the extract, ameliorated the kidney hypertrophy index in streptozotocin-induced diabetic rats (Alaofi 2020), and reduced the renal impairment and structural injuries (Ansari et al. 2017). Moreover, resveratrol exerted nephroprotection against MTX-induced toxicity through anti-nitrosative and anti-apoptotic effects, as well as

via upregulation of renal BCRP. Furthermore, umbelliferone protected against Cisp-induced nephrotoxicity in rats, as it could inhibit oxidative stress injury. Besides, umbelliferone significantly inhibited the inflammatory burden through suppression of NF-KB-p65/TNF- $\alpha$ /IL-1 $\beta$  expressions (Ali et al. 2021). Likewise, quercetin protected against kidney damage and reversed the renal weight loss, both, induced by NTiO<sub>2</sub>, which has a toxic effect on the kidney. It also reduced the cortical damage induced by cisplatin; however, it did not affect medullary damage (Casanova et al., 2021b). Finally, *Acacia hydas-pica*, *Globularia alypum*, *Anogeissus latifolia*, and *Azima tetracantha* extracts exerted similar activities (Sharma et al. 2021; Konda et al. 2016; Afsar et al. 2020; Feriani et al., 2017).

## 5. Conclusions

The present outcome is the first to deliver proof that aqueous extract of aerial parts of *M. ferruginea* revealed a beneficial effect on cisplatin-induced nephrotoxicity. The nephroprotective effect could be accredited to the anti-inflammatory and antioxidant phytochemicals of MF extract. Further research is needed to confirm the outlined activities as well as to isolate the individual components of the extract and explore their potential protective activities and mechanism of action.

## Declaration of Competing Interest

The authors declare that they have no known competing financial interests or personal relationships that could have appeared to influence the work reported in this paper.

## Acknowledgments

The authors are grateful for Prof. Farghaly A. Omar, Faculty of Pharmacy, Assiut University, Assiut, Egypt for performing the docking analysis and for Prof. Wink, Heidelberg University, for giving us the opportunity to collect LC-MS data.

## References

- Aebi, H., 1984. Catalase in vitro. In: *Methods in Enzymology*. Elsevier, pp. 121–126.
- Afsar, T., Razak, S., Aldisi, D., Shabbir, M., Almajwal, A., Al Kheraif, A.A., Arshad, M., 2021. *Acacia hydas-pica* R. parker ethyl-acetate extract abrogates cisplatin-induced nephrotoxicity by targeting ROS and inflammatory cytokines. *Sci. Rep.* 11, 1–16.
- Afsar, T., Razak, S., Almajwal, A., Al-Disi, D., 2020. Doxorubicin-induced alterations in kidney functioning, oxidative stress, dna damage, and renal tissue morphology; improvement by *Acacia hydas-pica* tannin-rich ethyl acetate fraction. *Saudi J. Biol. Sci.* 27, 2251–2260. <https://doi.org/10.1016/j.sjbs.2020.07.011>.
- Alaofi, A.L., 2020. Sinapic acid ameliorates the progression of streptozotocin (STZ)-Induced Diabetic Nephropathy in Rats via NRF2/HO-1 Mediated Pathways. *Front. Pharmacol.* 11, 1119. <https://doi.org/10.3389/fphar.2020.01119>.
- Ali, F.E.M., Hassanein, E.H.M., El-Bahrawy, A.H., Omar, Z.M.M., Rashwan, E.K., Abdel-Wahab, B.A., Abd-Elhamid, T.H., 2021. Nephroprotective effect of umbelliferone against cisplatin-induced kidney damage is mediated by regulation of NRF2, cytoglobin, SIRT1/FOXO-3, and NF- K B-p65 signaling pathways. *J. Biochem. Mol. Toxicol.* 35. <https://doi.org/10.1002/jbt.22738>.
- Ansari, M.A., Raish, M., Ahmad, A., Alkharfy, K.M., Ahmad, S.F., Attia, S.M., Alsaad, A.M.S., Bakheet, S.A., 2017. Sinapic acid ameliorate cadmium-induced nephrotoxicity: in vivo possible involvement of oxidative stress, apoptosis, and inflammation via NF-KB downregulation. *Environ. Toxicol. Pharmacol.* 51, 100–107. <https://doi.org/10.1016/j.etap.2017.02.014>.
- Arya, A., Jamil Al-Obaidi, M.M., Shahid, N., Bin Noordin, M.I., Looi, C.Y., Wong, W.F., Khaing, S.L., Mustafa, M.R., 2014. Synergistic effect of quercetin and quinic acid by alleviating structural degeneration in the liver, kidney and pancreas tissues of stz-induced diabetic rats: A mechanistic study. *Food Chem. Toxicol.* 71, 183–196. <https://doi.org/10.1016/j.fct.2014.06.010>.
- Bahiru, M., Tafesse, G., Chauhan, N.M., Assefa, E., 2020. Antimicrobial activity of crude extract from *Milletia ferruginea* leaves and barks against selected bacterial pathogens and *Candida albicans*. *JMAA* 12, 81–87.
- Bradford, M.M., 1976. A rapid and sensitive method for the quantitation of microgram quantities of protein utilizing the principle of protein-dye binding. *Anal. Biochem.* 72, 248–254. [https://doi.org/10.1016/0003-2697\(76\)90527-3](https://doi.org/10.1016/0003-2697(76)90527-3).
- Buege, J.A., Aust, S.D., 1978. Microsomal lipid peroxidation. In: *Methods in Enzymology*. Elsevier, pp. 302–310.
- Buyinza, D., Chalo, D.M., Derese, S., Ndakala, A., Yenesew, A., 2020. Flavonoids and isoflavonoids of *Milletia dura* and *Milletia ferruginea*: Phytochemical review and chemotaxonomic values. *Biochem. Sys. Ecol.* 91. <https://doi.org/10.1016/j.bse.2020.104053>.
- Casanova, A.G., Harvat, M., Vicente-Vicente, L., Pellicer-Valero, Ó. J., Morales, A.I., López-Hernández, F.J., Martín-Guerrero, J.D., 2021a. Regression modeling of the antioxidant-to-nephroprotective relation shows the pivotal role of oxidative stress in cisplatin nephrotoxicity. *Antioxidants* 10, 1355.
- Casanova, A.G., Prieto, M., Colino, C.I., Gutiérrez-Millán, C., Ruszkowska-Ciastek, B., de Paz, E., Martín, Á., Morales, A.I., López-Hernández, F.J., 2021b. A Micellar formulation of quercetin prevents cisplatin nephrotoxicity. *IJMS* 22, 729. <https://doi.org/10.3390/ijms22020729>.
- Choudhury, M.K., Shiferaw, Y., Sur, K.R., Dey, D., Debnath, S., Ghosh, S., Ray, R., Hazra, B., 2016. Antimicrobial activity and dna-fragmentation effect of isoflavonoids isolated from seeds of *Milletia ferruginea*, and endemic legume tree in Ethiopia. *J. Coast. Life Med.* 4, 556–563.
- Dhibi, S., Bouzenna, H., Samout, N., Tlili, Z., Elfeki, A., Hfaiedh, N., 2016. Nephroprotective and antioxidant properties of *Artemisia arborescens* hydroalcoholic extract against oestrogen-induced kidney damages in rats. *Biomed. Pharmacoth.* 82, 520–527. <https://doi.org/10.1016/j.biopha.2016.05.020>.
- Domitrović, R., Cvijanović, O., Pernjak-Pugel, E., Škoda, M., Mikielić, L., Crnčević-Orlić, Ž., 2013. Berberine exerts nephroprotective effect against cisplatin-induced kidney damage through inhibition of oxidative/nitrosative stress, inflammation, autophagy and apoptosis. *Food Chem. Toxicol.* 62, 397–406. <https://doi.org/10.1016/j.fct.2013.09.003>.
- El-Desouky, M.A., Mahmoud, M.H., Riad, B.Y., Taha, Y.M., 2019. Nephroprotective effect of green tea, rosmarinic acid and rosemary on n-diethylnitrosamine initiated and ferric nitrilotriacetate promoted acute renal toxicity in wistar rats. *Interdiscip. Toxicol.* 12, 98–110. <https://doi.org/10.2478/intox-2019-0012>.
- El-Hawary, S.S., Sobeh, M., Badr, W.K., Abdelfattah, M.A.O., Ali, Z. Y., El-Tantawy, M.E., Rabeh, M.A., Wink, M., 2020. HPLC-PDA-MS/MS profiling of secondary metabolites from *Opuntia ficus-indica* cladode, peel and fruit pulp extracts and their antioxidant, neuroprotective effect in rats with aluminum chloride induced neurotoxicity. *Saudi J. Biol. Sci.* 27, 2829–2838. <https://doi.org/10.1016/j.sjbs.2020.07.003>.
- Erdemli, Z., Erdemli, M.E., Gul, M., Altinoz, E., Gul, S., Kocaman, G., Kustepe, E.K., Bag, H.G., 2021. Ameliorative effects of crocin

- on the inflammation and oxidative stress-induced kidney damages by experimental periodontitis in rat. *Iran J. Basic Med. Sci.* 24, 825.
- Fang, C., Lou, D., Zhou, L., Wang, J., Yang, B., He, Q., Wang, J., Weng, Q., 2021. Natural products: Potential treatments for cisplatin-induced nephrotoxicity. *Acta Pharmacol. Sin.* <https://doi.org/10.1038/s41401-021-00620-9>.
- Feriani, A., del Mar Contreras, M., Talhaoui, N., Gómez-Caravaca, A.M., Taamalli, A., Segura-Carretero, A., Ghazouani, L., El Feki, A., Allagui, M.S., 2017. Protective effect of *Globularia alypum* leaves against deltamethrin-induced nephrotoxicity in rats and determination of its bioactive compounds using high-performance liquid chromatography coupled with electrospray ionization tandem quadrupole–time-of-flight mass spectrometry. *J. Func. Foods* 32, 139–148. <https://doi.org/10.1016/j.jff.2017.02.015>.
- Flohé, L., Günzler, W.A., 1984. *Assays of Glutathione Peroxidase. In: Methods in Enzymology.* Elsevier, pp. 114–120.
- Ghareeb, M.A., Mohamed, T., Saad, A.M., Refahy, L.-A.-G., Sobeh, M., Wink, M., 2018. HPLC-DAD-ESI-MS/MS analysis of fruits from *Firmiana simplex* (L.) and evaluation of their antioxidant and antigenotoxic properties. *J. Pharm. Pharmacol.* 70, 133–142.
- Hussain, T., Gupta, R.K., Sweetey, K., Eswaran, B., Vijayakumar, M., Rao, C.V., 2012. Nephroprotective activity of *Solanum xanthocarpum* fruit extract against gentamicin-induced nephrotoxicity and renal dysfunction in experimental rodents. *Asian Pac. J. Trop. Med.* 5, 686–691. [https://doi.org/10.1016/S1995-7645\(12\)60107-2](https://doi.org/10.1016/S1995-7645(12)60107-2).
- Kanno, S., Shouji, A., Hirata, R., Asou, K., Ishikawa, M., 2004. Effects of naringin on cytosine arabinoside (ARA-C)-induced cytotoxicity and apoptosis in p388 cells. *Life Sci.* 75, 353–365. <https://doi.org/10.1016/j.lfs.2003.12.019>.
- Kim, T.-W., Kim, Y.-J., Seo, C.-S., Kim, H.-T., Park, S.-R., Lee, M.-Y., Jung, J.-Y., 2016. *Elsholtzia ciliata* (Thunb.) hylander attenuates renal inflammation and interstitial fibrosis via regulation of TGF- $\beta$  and Smad3 expression on unilateral ureteral obstruction rat model. *Phytomed* 23, 331–339.
- Konda, V.R., Arunachalam, R., Eerike, M., Rao, K.R., Radhakrishnan, A.K., Raghuraman, L.P., Meti, V., Devi, S., 2016. Nephroprotective Effect of Ethanolic Extract of Azima Tetracantha Root in Glycerol Induced Acute Renal Failure in Wistar Albino Rats. *J. Trad. Complement. Med.* 6, 347–354. <https://doi.org/10.1016/j.jtcm.2015.05.001>.
- Lim, Y.J., Sidor, N.A., Toniai, N.C., Che, A., Urquhart, B.L., 2021. Uremic toxins in the progression of chronic kidney disease and cardiovascular disease: Mechanisms and therapeutic targets. *Toxins* 13, 142. <https://doi.org/10.3390/toxins13020142>.
- Marklund, S., Marklund, G., 1974. Involvement of the superoxide anion radical in the autoxidation of pyrogallol and a convenient assay for superoxide dismutase. *Eur. J. Biochem.* 47, 469–474. <https://doi.org/10.1111/j.1432-1033.1974.tb03714.x>.
- Nibret, E., Wink, M., 2011. Trypanocidal and cytotoxic effects of 30 Ethiopian medicinal plants. *Z. Naturforsch. C* 66, 541–546.
- Rehman, M.U., Ali, N., Rashid, S., Jain, T., Nafees, S., Tahir, M., Khan, A.Q., Lateef, A., Khan, R., Hamiza, O.O., 2014. Alleviation of hepatic injury by chrysin in cisplatin administered rats: probable role of oxidative and inflammatory markers. *Pharmacol. Rep.* 66, 1050–1059.
- Rehman, M.U., Rather, I.A., 2019. Myricetin abrogates cisplatin-induced oxidative stress, inflammatory response, and goblet cell disintegration in colon of wistar rats. *Plants* 9, 28.
- Rjeibi, I., Feriani, A., Ben Saad, A., Sdayria, J., Saidi, I., Ncib, S., Souid, S., Allagui, M.S., Hfaiedh, N., 2018. *Lycium europaeum* extract: A new potential antioxidant source against cisplatin-induced liver and kidney injuries in mice. *Oxid. Med. Cell. Longev.* 2018, 1–9. <https://doi.org/10.1155/2018/1630751>.
- Sahu, B.D., Kuncha, M., Sindhura, G.J., Sistla, R., 2013. Hesperidin attenuates cisplatin-induced acute renal injury by decreasing oxidative stress, inflammation and DNA damage. *Phytomed* 20, 453–460. <https://doi.org/10.1016/j.phymed.2012.12.001>.
- Sancak, E.B., Akbas, A., Silan, C., Cakir, D.Ü., Sidika Seyma, O., 2016. Syringic acid preconditioning improves kidney ischemia-reperfusion. *Europ. Urol. Supp.* 15, [https://doi.org/10.1016/S1569-9056\(16\)60604-8](https://doi.org/10.1016/S1569-9056(16)60604-8) e602.
- Sellins, K.S., Cohen, J.J., 1995. Nuclear Changes in the Cytotoxic T Lymphocyte-Induced Model of Apoptosis. *Immunol. Rev.* 146, 241–266. <https://doi.org/10.1111/j.1600-065X.1995.tb00692.x>.
- Sharma, V.C., Kaushik, A., Dey, Y.N., Srivastava, B., Wanjari, M., Pawar, S., Chougule, S., 2021. Nephroprotective potential of *Anogeissus latifolia* Roxb. (Dhava) against gentamicin-induced nephrotoxicity in rats. *J. Ethnopharmacol.* 273, <https://doi.org/10.1016/j.jep.2021.114001> 114001.
- Speeckaert, M.M., Speeckaert, R., Laute, M., Vanholder, R., Delanghe, J.R., 2012. Tumor necrosis factor receptors: Biology and therapeutic potential in kidney diseases. *Am. J. Nephrol.* 36, 261–270. <https://doi.org/10.1159/000342333>.
- Taguchi, S., Azushima, K., Yamaji, T., Urate, S., Suzuki, T., Abe, E., Tanaka, S., Tsukamoto, S., Kamimura, D., Kinguchi, S., et al., 2021. Effects of tumor necrosis factor- $\alpha$  inhibition on kidney fibrosis and inflammation in a mouse model of aristolochic acid nephropathy. *Sci. Rep.* 11, 23587. <https://doi.org/10.1038/s41598-021-02864-1>.
- Tir, M., Feriani, A., Labidi, A., Mufti, A., Saadaoui, E., Nasri, N., Khaldi, A., El Cafsi, M., Tlili, N., 2019. Protective effects of phytochemicals of *Capparis spinosa* seeds with cisplatin and CCl4 toxicity in mice. *Food Biosci.* 28, 42–48. <https://doi.org/10.1016/j.fbio.2019.01.002>.
- Tlili, N., Feriani, A., Saadoui, E., Nasri, N., Khaldi, A., 2017. *Capparis spinosa* leaves extract: source of bioantioxidants with nephroprotective and hepatoprotective effects. *Biomed. Pharmacoth.* 87, 171–179. <https://doi.org/10.1016/j.biopha.2016.12.052>.
- Wang, Y.-Y., Kwak, J.H., Lee, K.-T., Deyou, T., Jang, Y.P., Choi, J.-H., 2020. Isoflavones isolated from the seeds of *Millettia ferruginea* induced apoptotic cell death in human ovarian cancer cells. *Molecules* 25, 207.